Supplementary materials

1 Materials

$Ni(CH_3COO)_2·4H_2O$, $NiCl_2·6H_2O$, $NiSO_4·6H_2O$, $Ni(NO_3)_2·6H_2O$ and $C_2H_4N_4$ were purchased from Tianjin Chemical Corporation. Sulfuric acidic (H_2SO_4, AR) and potassium hydroxide (KOH, AR), PVDF, and anhydrous ethanol were purchased from Liaoning Quanrui Reagent Co. Ltd. Carbon paper was purchased from Hesen Electric Co. Ltd. (Shanghai, China). The commercial graphite rod, Hg/HgO electrode, and Ag/AgCl electrode were acquired from AIDA Science-Technology Development Co. Ltd. (Tianjin, China). We utilized ultrapure water to prepare all the aqueous solutions.

2 Structure characterization

SEM images were taken using a Rigaku S-4300 operating. TEM images were obtained by using a HITACHI H-7650 transmission electron microscope and Gatan imaging filter (GIF). XPS data were acquired using a Thermo ESCALAB250 X-ray photoelectron spectrometer. X-ray diffraction (XRD) data were collected at room temperature with a 2θ scan range of 10°–90° using an X-ray diffractometer (PANalytical) equipped with Cu K_α radiation (1.54 Å).

3 Electrochemical measurements

Electrochemical measurements were conducted in a three-electrode system with an electrochemical station (CHI660E, CH Instrument, USA). Three electrodes consisting of carbon paper as the working electrode (1 cm^2) and a graphite rod and a Hg/HgO (KOH saturated) as counter and reference electrodes were used. The preparation of the working electrode is described below: the catalysts were dispersed in N-methyl-2-pyrrolidone solvent containing 7.5 wt% PVDF under sonication, in which the weight ratio of the catalyst to PVDF was 8: 1. Then the slurry was coated onto a piece of carbon paper. The loading mass of the catalysts was approximately 3.5 mg/cm^2 for all the working electrodes. N_2-saturated electrolytes, including 1.0 mol/L KOH, were used to examine the electrocatalytic activities of the catalysts for HER and OER. Linear sweep voltammetry (LSV) at a scanning rate of 5 mV/s was utilized to get polarization curves. The chronoamperometry measurements were adopted to conduct the test features' long-term stability. The equation adopted to calibrate all the measured potentials to RHE is as follows:

$$E(\text{vs RHE})=E(\text{Hg/HgO})+0.098+0.059\text{pH} \quad \text{(S1)}$$

The compensated potential was corrected using the equation $E_{\text{compensated}}=E_{\text{measured}}-IR$, where $E_{\text{compensated}}$ and E_{measured} denote the compensated and measured potentials, respectively.

4 Turnover frequency (TOF) calculation

The number of active sites (n) was first examined employing cyclic voltammograms with a phosphate buffer (pH=7) at a scan rate of 50 mV/s. Then, the number of the voltammetric charges (Q) could be determined after the deduction of the blank value. n could be determined with the following equation:

$$n=Q/(2F) \text{ (HER)} \quad \text{(S2)}$$

$$n=Q/(4F) \text{ (OER)} \quad \text{(S3)}$$

where F is the Faraday constant.

TOF could be calculated with Eqs. (5) and (6).

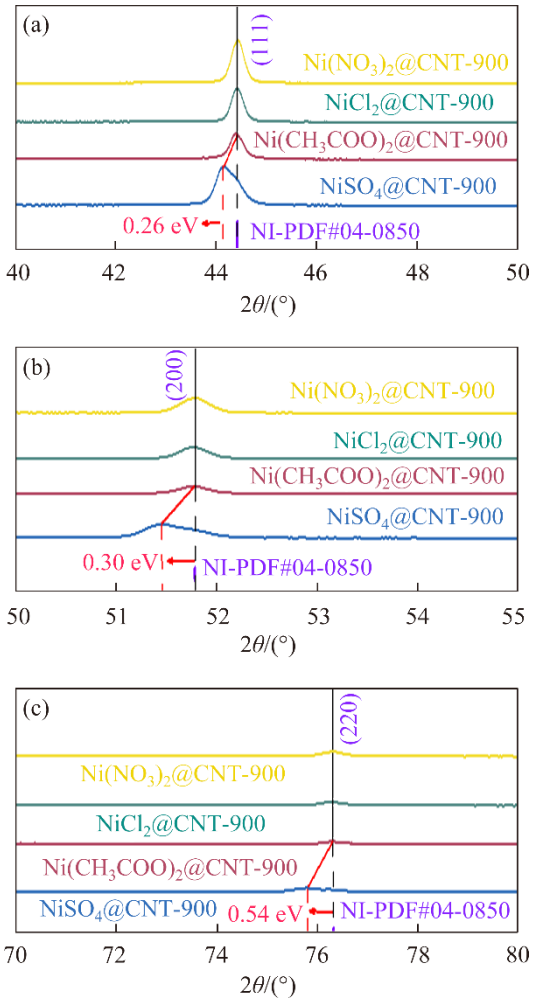

Figure S1 Detailed comparisons of the planes peak positions of Ni for $Ni(NO_3)_2$@CNT-900, $NiCl_2$@CNT-900, $Ni(CH_3COO)_2$@CNT-850, and $NiSO_4$@CNT-900: (a) (111); (b) (200); (c) (220)

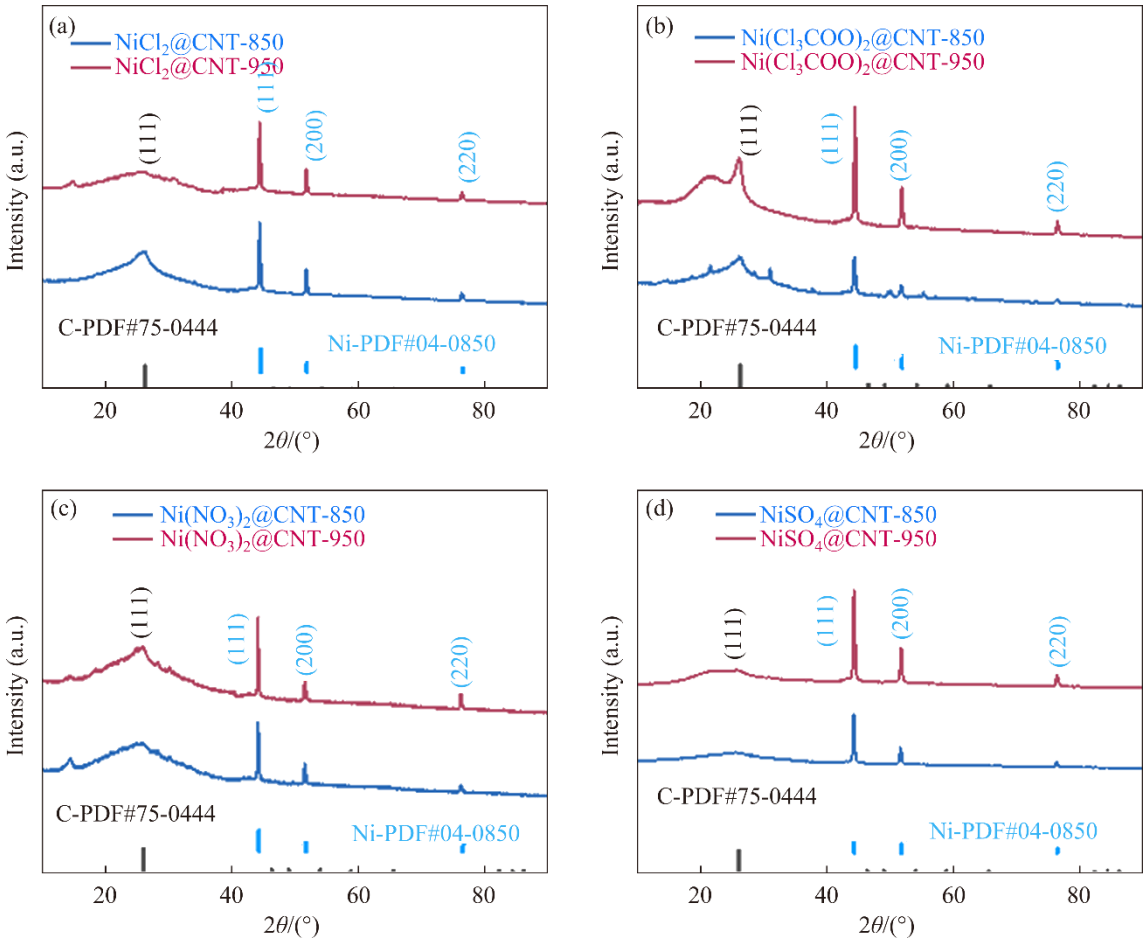

Figure S2 XRD patterns of: (a) $NiCl_2$@CNT-850/950; (b) $Ni(CH_3COO)_2$@CNT-850/950; (c) $Ni(NO_3)_2$@CNT-850/950; (d) $NiSO_4$@CNT-850/950

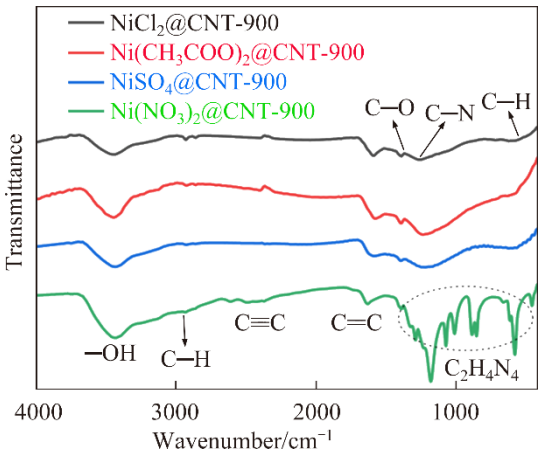

Figure S3 FT-IR pattern of $NiCl_2$@CNT-900, $Ni(CH_3COO)_2$@CNT-900, $Ni(NO_3)_2$@CNT-900, $NiSO_4$@CNT-900

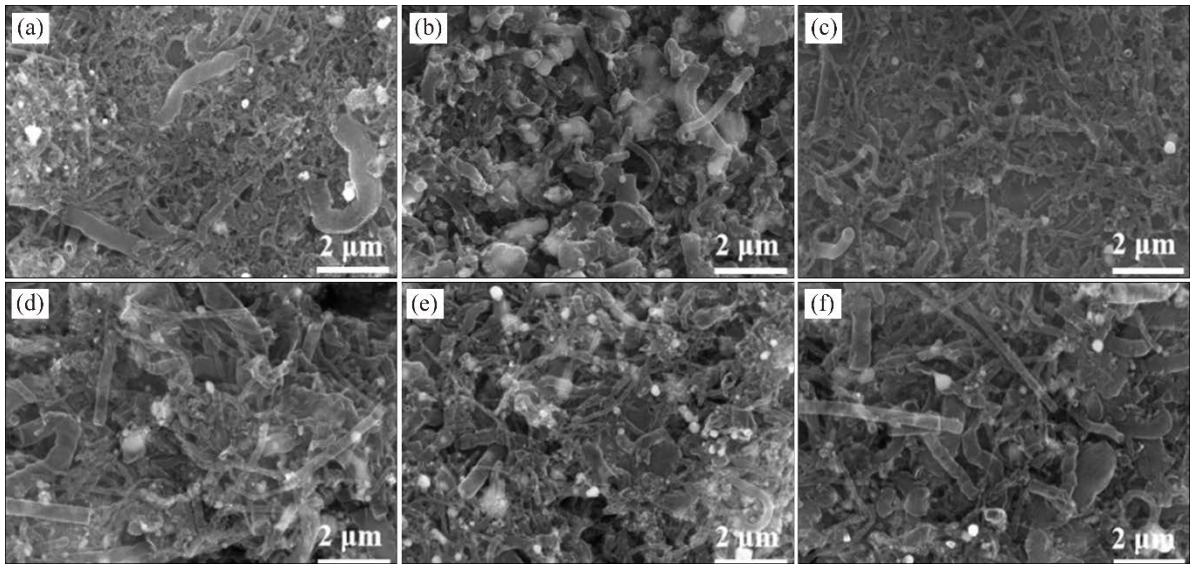

Figure S4 SEM images of: (a) $Ni(NO_3)_2$@CNT-850; (b) $Ni(NO_3)_2$@CNT-900; (c) $Ni(NO_3)_2$@CNT-950; (d) $NiSO_4$@CNT-850; (e) $NiSO_4$@CNT-900; (f) $NiSO_4$@CNT-950

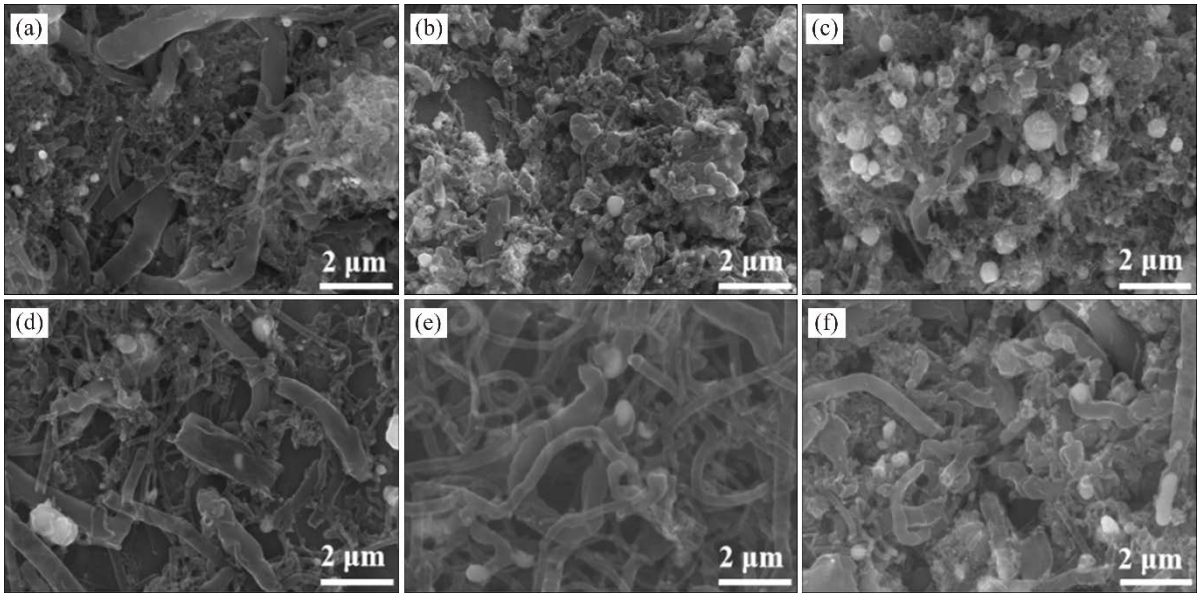

Figure S5 SEM images of: (a) $NiCl_2$@CNT-850; (b) $NiCl_2$@CNT-900; (c) $NiCl_2$@CNT-950; (d) $Ni(CH_3COO)_2$@CNT-850; (e) $Ni(CH_3COO)_2$@CNT-900; (f) $Ni(CH_3COO)_2$@CNT-950

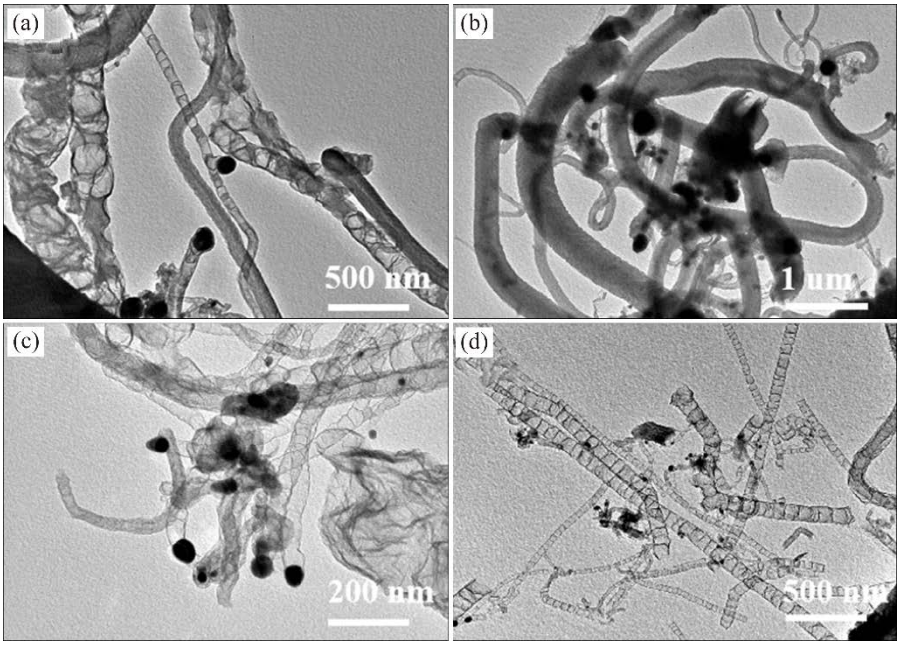

Figure S6 TEM images of: (a) $Ni(NO_3)_2$@CNT-900; (b) $NiSO_4$@CNT-900; (c) $NiCl_2$@CNT-900; (d) $Ni(CH_3COO)_2$@CNT-900

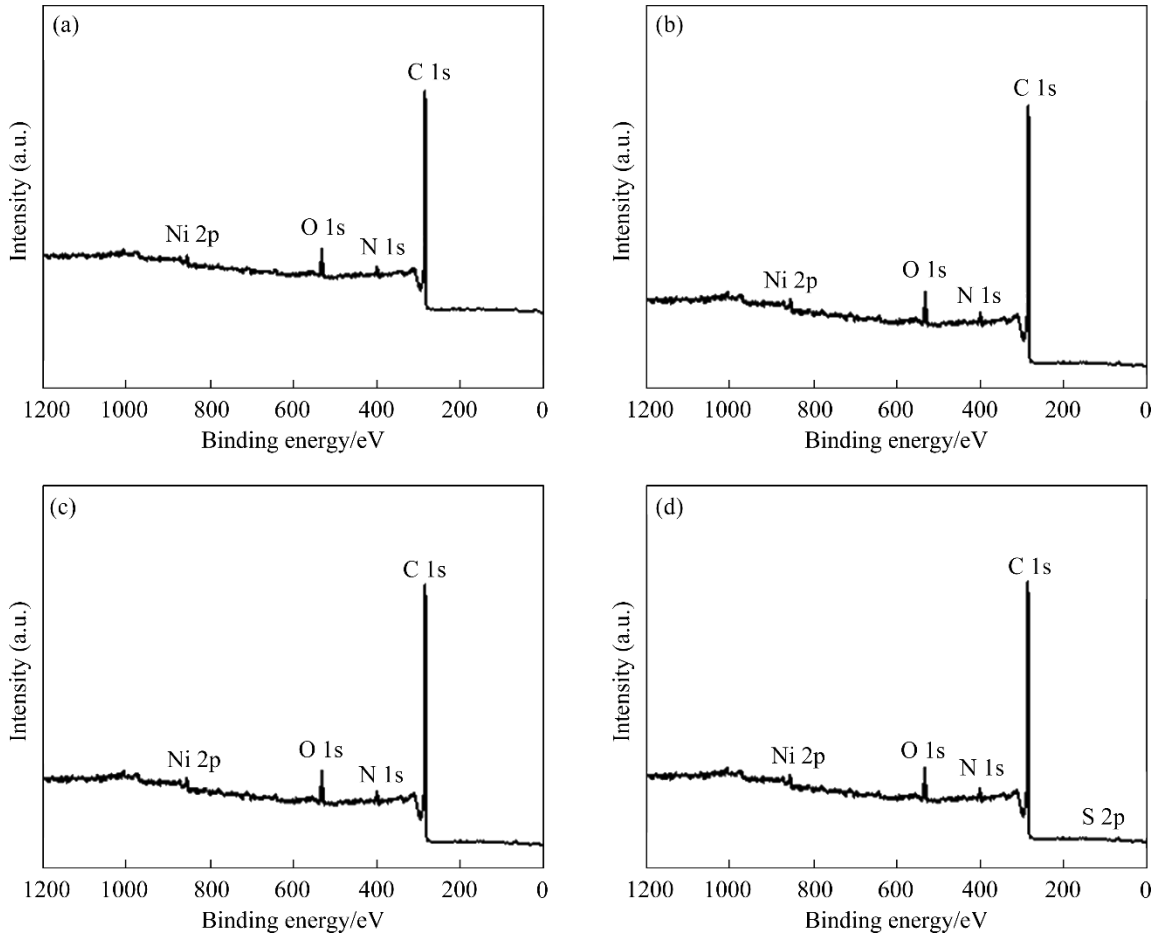

Figure S7 XPS spectra survey of the bimetallic NiX@CNT-900 catalysts: (a) $Ni(NO_3)_2$@CNT-900; (b) $NiCl_2$@CNT-900; (c) $Ni(CH_3COO)_2$@CNT-900; (d) $NiSO_4$@CNT-900

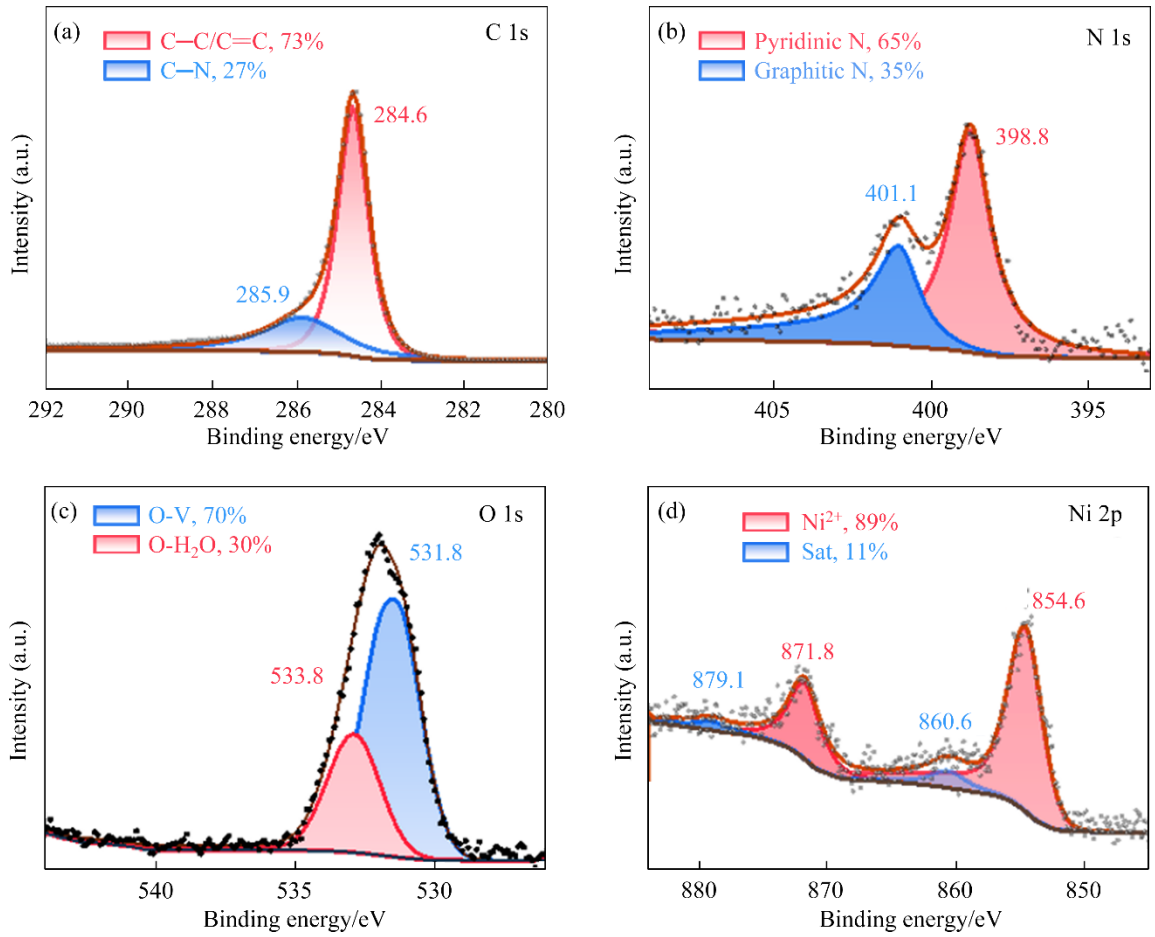

Figure S8 XPS spectra of the bimetallic $NiCl_2$@CNT-900 catalysts: (a) C 1s; (b) N 1s; (c) O 1s; (d) Ni 2p

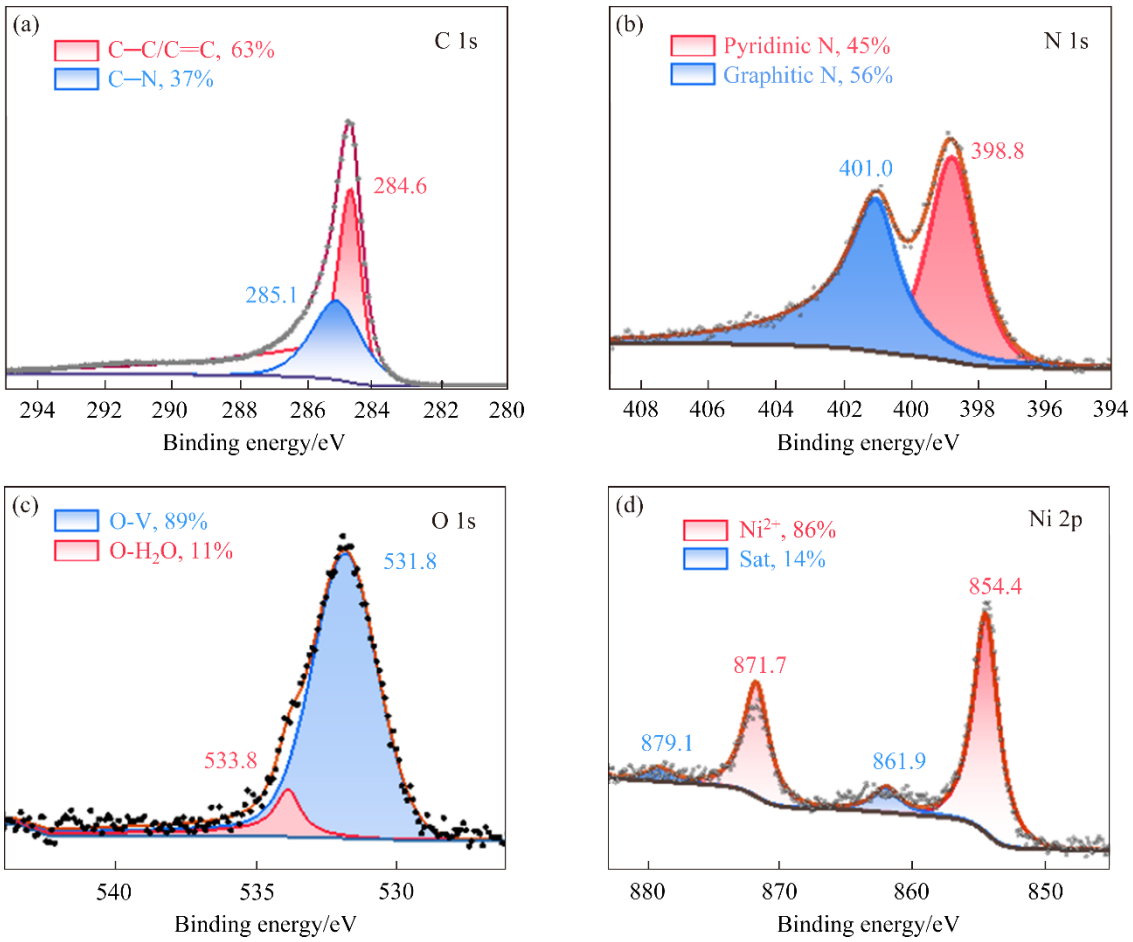

Figure S9 XPS spectra of the bimetallic $Ni(CH_3COO)_2$@CNT-900 catalysts: (a) C 1s; (b) N 1s; (c) O 1s; (d) Ni 2p

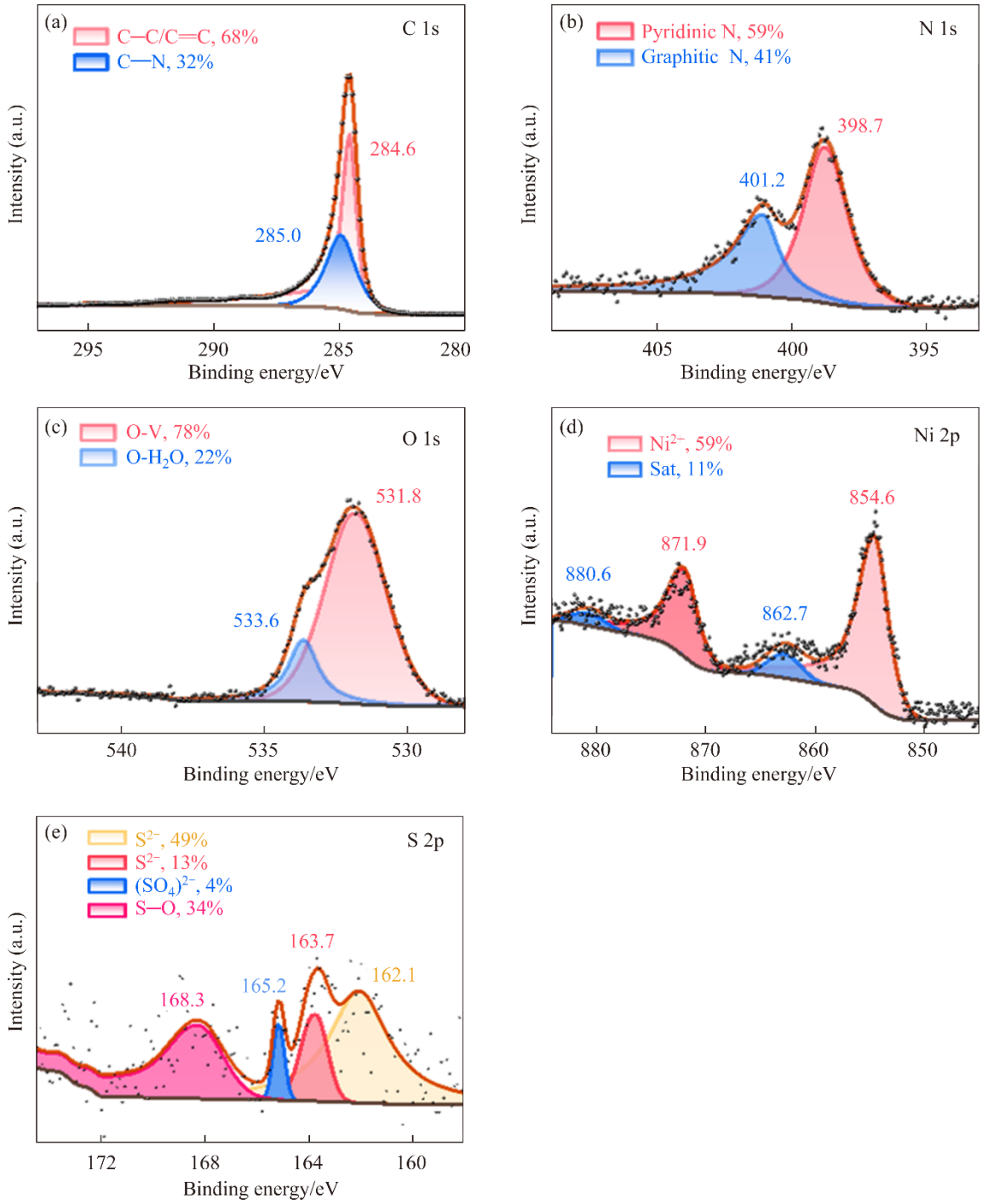

Figure S10 XPS spectra of the bimetallic $NiSO_4$@CNT-900 catalysts: (a) C 1s; (b) N 1s; (c) O 1s; (d) Ni 2p; (e) S 2p

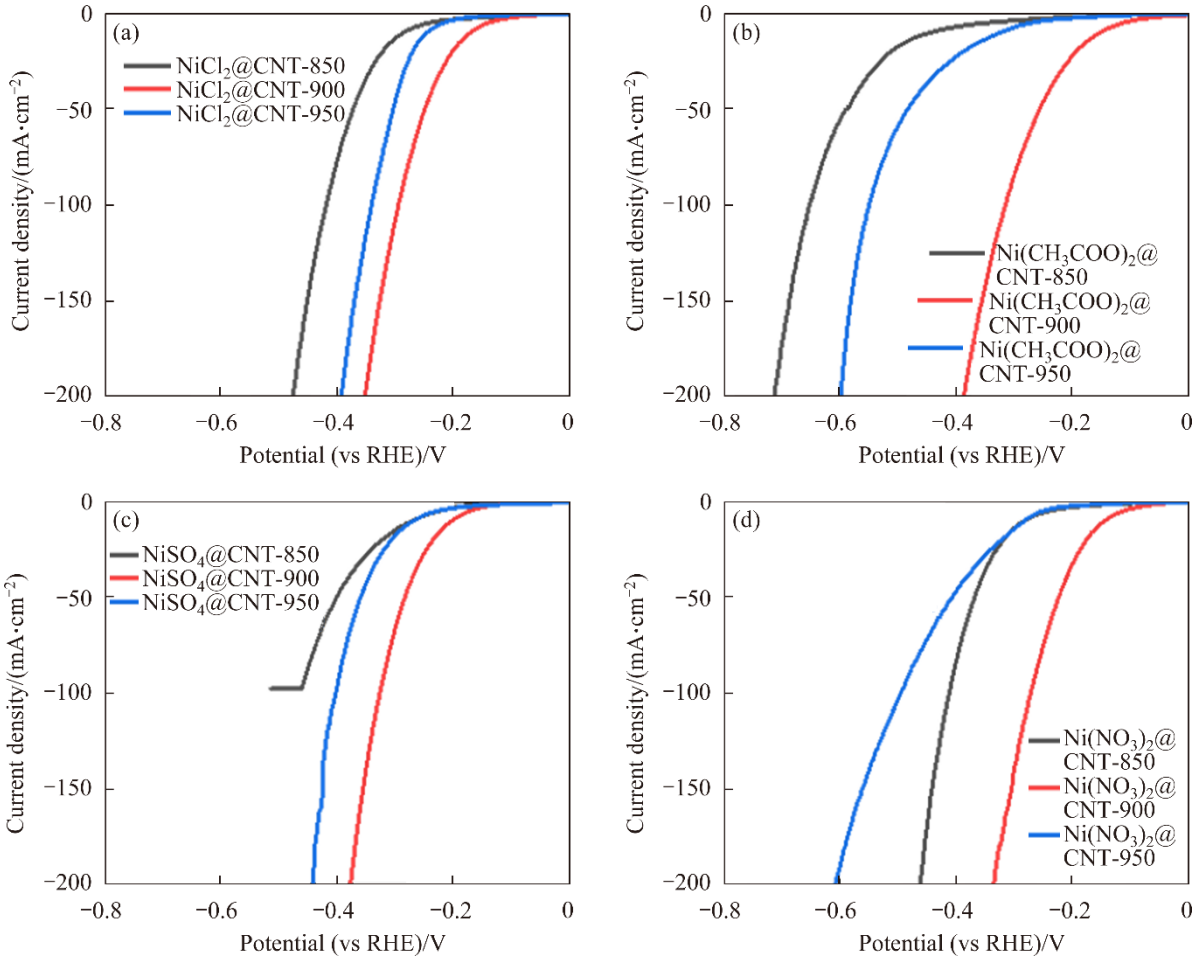

Figure S11 The polarization curves of (a)$NiCl_2$@CNT, (b) $Ni(CH_3COO)_2$@CNT, (c) $NiSO_4$@CNT and (d) $Ni(NO_3)_2$@CNT in 1 mol/L KOH

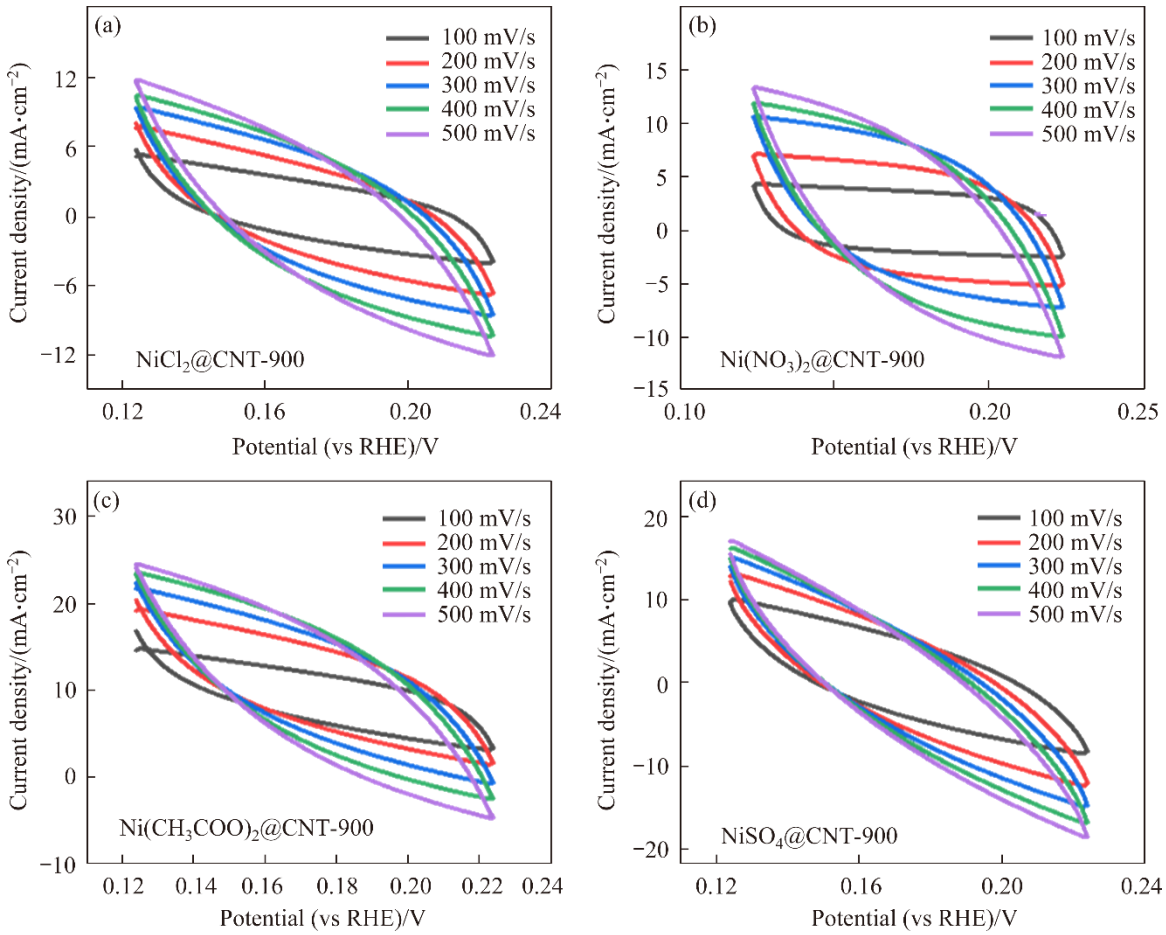

Figure S12 CV_{HER} curves of $NiCl_2$@CNT-900 electrode (a), $Ni(NO_3)_2$@CNT-900 electrode (b), $Ni(CH_3COO)_2$@CNT-900 electrode (c) and $NiSO_4$@CNT-900 electrode (d) in non-Faradaic region under different scan rates

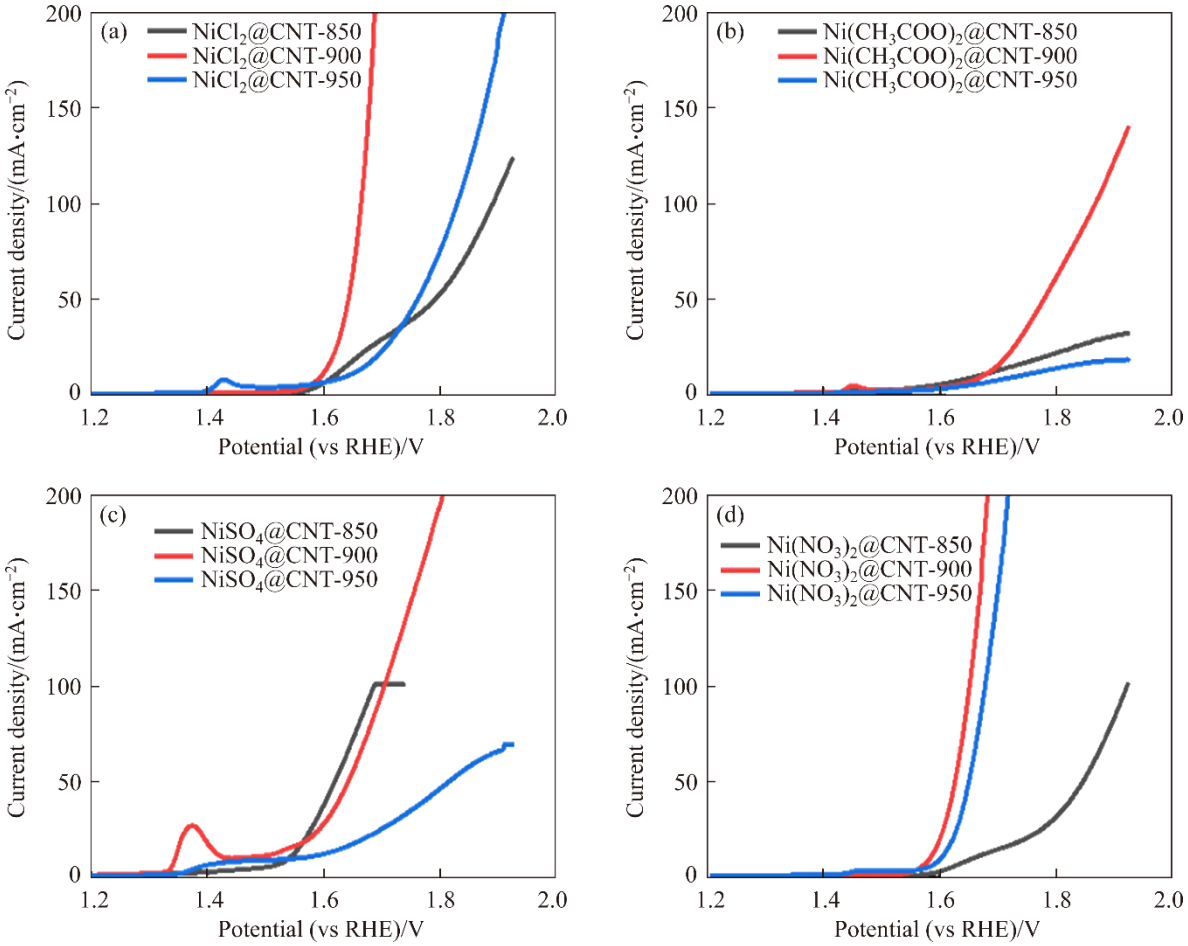

Figure S13 The polarization curves of (a) $NiCl_2$@CNT, (b) $Ni(CH_3COO)_2$@CNT, (c) $NiSO_4$@CNT and (d) $Ni(NO_3)_2$@CNT in 1 mol/L KOH

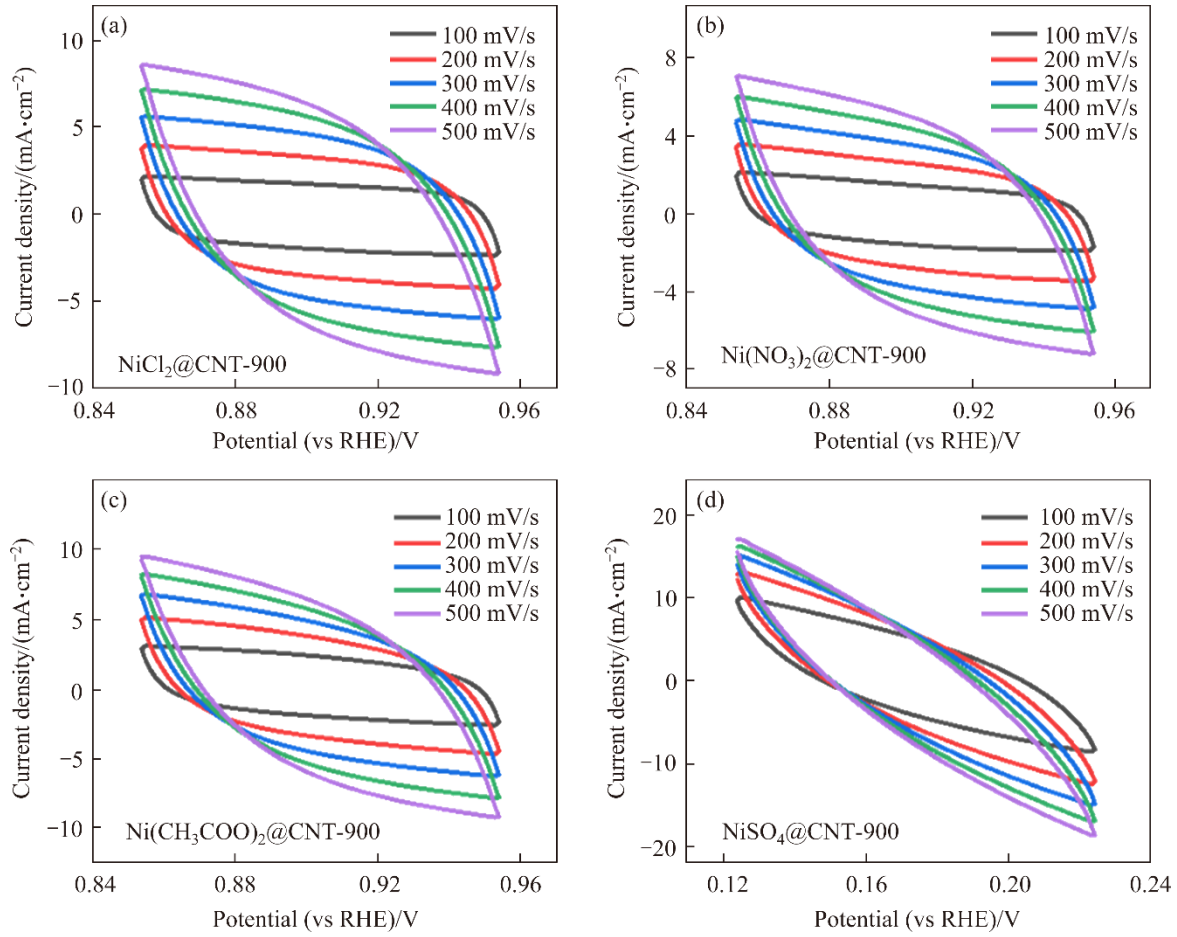

Figure S14 CV_{OER} curves of $NiCl_2$@CNT-900 electrode (a), $Ni(NO_3)_2$@CNT-900 electrode(b), $Ni(CH_3COO)_2$@CNT-900 electrode (c) and $NiSO_4$@CNT-900 electrode(d) in the non-faradaic region under different scan rates

Table S1 Comparison of the HER, Tafel, impedance values of the prepared materials

Sample	Overpotential at 10 mA/cm^2 (vs RHE)/mV	Tafel slop/(mV·dec^{-1})	Impedance/Ω
$NiCl_2$@CNT-850	283	126.6	2.13
$NiCl_2$@CNT-900	169	122.4	1.85
$NiCl_2$@CNT-950	244	88.1	2.35
$Ni(CH_3COO)_2$@CNT-850	441	205.9	2.56
$Ni(CH_3COO)_2$@CNT-900	151	158.7	2.01
$Ni(CH_3COO)_2$@CNT-950	332	226.9	2.48
$Ni(NO_3)_2$@CNT-850	282	131.1	1.96
$Ni(NO_3)_2$@CNT-900	145	112.2	1.79
$Ni(NO_3)_2$@CNT-950	293	258.3	2.08
$NiSO_4$@CNT-850	275	191.8	2.05
$NiSO_4$@CNT-900	206	117.9	2.27
$NiSO_4$@CNT-950	272	127.3	2.19

Table S2 Comparison of the HER of the $Ni(NO_3)_2$@CNT-900 based electrode in this work with other related alloy materials

Sample	Overpotential at 10 mA/cm^2 (vs RHE)/mV	Reference
$Ni(NO_3)_2$@CNT-900	145	This work
Fe-Ni-Co	178	[3]
NiMoN	191	[21]
$Fe_{0.6}Co_{0.4}$-P	346	[36]
NiFe-NiFeP@NC/CNT	228	[39]
g-C_3N_4 QDs	208	[43]
Ni-Mo_xC-NC	162	[44]
NiFeMo/NF	180	[45]
$Co_1Fe_1Mo_{1.8}O$ NMs@NF	157	[46]
Ni@NC	190	[47]
Co@BCN	183	[48]
Co−P/NC	191	[49]

Table S3 Comparison of the OER, Tafel, impedance values of the prepared materials

Sample	Overpotential at 10 mA/cm^2 (vs RHE)/mV	Tafel slop/(mV·dec^{-1})	EIS/Ω
$NiCl_2$@CNT-850	387	109.8	1.68
$NiCl_2$@CNT-900	365	67.4	1.26
$NiCl_2$@CNT-950	409	168.6	1.49
$Ni(CH_3COO)_2$@CNT-850	448	291	1.59
$Ni(CH_3COO)_2$@CNT-900	444	155.5	1.47
$Ni(CH_3COO)_2$@CNT-950	506	329.7	1.79
$Ni(NO_3)_2$@CNT-850	429	237.6	1.76
$Ni(NO_3)_2$@CNT-900	300	67.3	1.15
$Ni(NO_3)_2$@CNT-950	374	76.7	1.98
$NiSO_4$@CNT-850	307	174.1	1.59
$NiSO_4$@CNT-900	332	178.2	1.33
$NiSO_4$@CNT-950	301	327.6	1.36

Table S4 Comparison of the OER of the $Ni(NO_3)_2$@CNT-900 based electrode in this work with other related alloy materials

Sample	Overpotential at 10 mA/cm^2 (vs RHE)/mV	Reference
$Ni(NO_3)_2$@CNT-900	300	This work
$Fe_{0.6}Co_{0.4}$-P	364	[36]
NiFe-NiFeP@NC/CNT	328	[39]
Ni-Mo_xC-NC	328	[44]
Co-Ni-P-2	340	[50]
Fe-CQDs/$NiMoO_4$/NF	336	[51]
C@$NiCo_{12}$	320	[52]
NiCo-300	320	[53]
FeCo-TA@CMS	380	[54]
NiCo-$NiCoO_2$@NC	318	[55]
N-rGO/CoFe-$CoFe_2O_4$	320	[25]